INTERNATIONAL JOURNAL FOR NUMERICAL METHODS IN FLUIDS
Int. J. Numer. Meth. Fluids 2009; **60**:323–336
Published online 29 July 2008 in Wiley InterScience (www.interscience.wiley.com). DOI: 10.1002/fld.1889

A new Navier–Stokes inverse method based on mass-averaged tangential velocity for blade design

M. T. Rahmati[1, 2, *, †]

[1]*Department of Mechanical Engineering, University College London, London, U.K.*
[2]*Engineering Department, Lancaster University, U.K.*

SUMMARY

This paper presents a novel viscous inverse method for blade design. In this inverse design method the mass-averaged tangential velocity and the blade thickness are prescribed, and the corresponding blade profile is sought. The blade profile is then computed iteratively using the discrepancies between the prescribed mass-averaged tangential velocity distribution and its calculated distribution on an initial blade. The re-design of an axial rotor blade, starting from an initial arbitrary profile in subsonic flow regimes, demonstrates the merits and robustness of this approach. Copyright © 2008 John Wiley & Sons, Ltd.

Received 4 July 2007; Revised 31 May 2008; Accepted 21 June 2008

KEY WORDS: inverse method; turbomachinery blade design; viscous flow; finite volume method

1. INTRODUCTION

A large number of robust and sophisticated flow analysis codes are now available for simulation of flow through turbomachinery blades [1–3]. These codes can be directly used for blade design based on 'trial-and-error' approaches. By guessing a blade shape, the flow solution can be obtained using the computation fluid dynamics (CFD) codes. The flow solution is then compared with the desired flow conditions. If these are not met then the blade geometry is altered. The whole process is repeated again, until the required flow conditions are achieved. In this design method, the designer relies on his previous experience to modify the blade shape at a certain location in order to improve the flow field there. However, there is always a risk that the modifications may have an adverse effect at other locations on the blade. Indeed, this approach to design relies on the designer's experience, talents, and creativity in reducing the number of trials needed before a successful final design is reached. Thus, these methods are very inefficient and time consuming.

*Correspondence to: M. T. Rahmati, Engineering Department, Lancaster University, U.K.
†E-mail: m.rahmati@lancs.ac.uk, mt.rahmati@googlemail.com

In order to reduce the development and design time and their associated costs, a more systematic method is required. The direct methods can be automated by coupling an automatic optimization algorithm, CAD-based blade generator, and a CFD code [4, 5]. In this method, the numerical analysis methods are coupled with a numerical optimization algorithm to maximize or minimize a design parameter. The prescribed design condition is arbitrary as long as they can be included in the objective function. Optimization methods for blade design are usually based on parametric definition of the blade geometry, either using surface definition or camber plus thickness. The surface is defined in terms of B-splines or Bezier curves with control points that can be modified by an optimization algorithm [4, 5]. Optimization methods can certainly reduce man costs if an efficient and high-performance flow analysis code and suitable optimization algorithms are used. These methods are, however, very expensive in terms of the required CPU, particularly, when they are coupled with a flow analysis algorithm based on the Navier–Stokes equations.

Inverse design method is an alternative method that defines the blade shape for a prescribed local flow property, such as surface pressure or velocity distribution. In comparison with optimization methods, inverse design methods allow a more direct interaction with the flow parameters and require much less efforts by the designer. Indeed, in these methods the physical model is used to drive the geometrical changes required for achieving the prescribed local flow quantity. Inverse methods directly define a geometry needed to obtain a prescribed target design parameter, which is related to the performance of turbomachinery or marine propeller blades. Indeed, these methods replace the time-consuming iterative procedure of direct methods in which a large number of different blade shapes are designed and analyzed to find the one which creates the blade velocity or pressure distribution closest to the desired one.

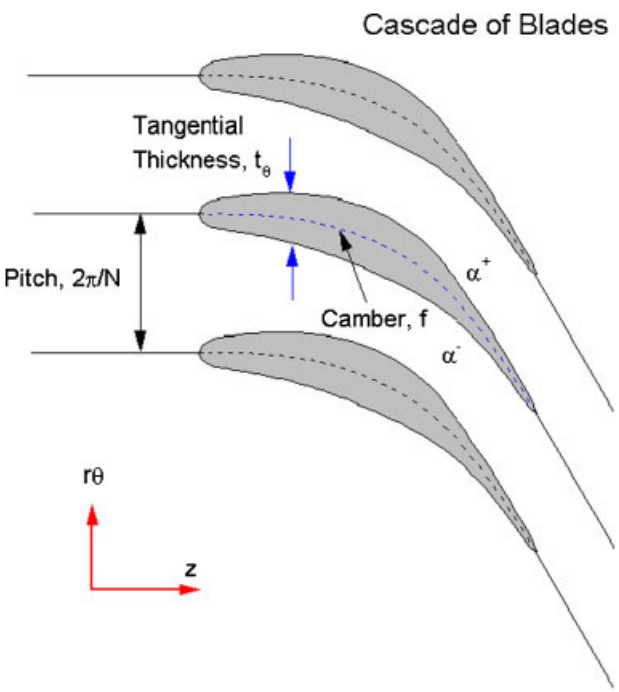

Figure 1. Blade cascade with prescribed tangential thickness.

DOI: 10.1002/fld

A pioneering inverse shape design method based on conformal mapping was proposed by Lighthill [6] in 1945. Since then, as a result of the continued commercial imperative to produce components of the highest quality in the shortest possible time, notable developments in the field of inverse design have been achieved. These inverse design methods are based on potential flow equations [7, 8] or Euler flow equations [9, 10]. The methods provide inviscid geometries so that many characteristics of real flow fields are ignored. The viscous effects predominate in the blade boundary layer, the wake regions, and the endwall regions of turbomachinery blades, which are the main cause for losses through skin friction on the blades. Moreover, the viscosity and turbulence affect tip vortex and secondary flow of turbomachinery blades which can have significant effects on the performance of turbomachinery. So, accurate modelling of viscous flow by utilizing Navier–Stokes equations is essential in order to design the blade or airfoil shape accurately [11].

Also the majority of inverse design methods are based on the prescription of surface pressure [9, 12]. These methods have the advantage that the designers have control over the flow field properties, such as blade surface pressure, which is related to aerodynamics performance of turbomachinery. However, the prescription of this condition may yield to unrealistic blades as shown by Rahmati [13] and Dang [14].

A pioneering inverse design based on the prescription of mass-averaged tangential velocity on the blade was proposed by Hawthrone *et al.* [15]. It was based on potential flow equations. This method was applied for the inverse design of a low-speed impeller by Borges [16] and for design of radial turbomachines in transonic flows by Zangeneh [8]. The method was extended to Euler flow equations by Dang and Jiang [10]. In this paper a new viscous design method based on the prescription of mass-averaged velocity is presented.

The mass-averaged tangential velocity, $r\tilde{V}_\theta$, for axial turbomachines is defined as follows:

$$r\tilde{V}_\theta = \frac{\int_{\theta\,\mathrm{upper}}^{\theta\,\mathrm{lower}} r V_\theta (\rho V_z)\,\mathrm{d}\theta}{\int_{\theta\,\mathrm{upper}}^{\theta\,\mathrm{lower}} (\rho V_z)\,\mathrm{d}\theta} \tag{1}$$

In this equation ρ is flow density, θ denotes the tangential coordinate of a cylindrical polar coordinates system, z denotes the axial direction, and r is the radius. The integral is made in the tangential direction from the upper surface of one blade, θ_{upper}, to lower surface of the next blade, θ_{lower}, see Figure 1. In Figure 1, N denotes the number of turbomachinery blades.

In this approach, the blade thickness and the mass-averaged tangential velocity along the blade surface of an initial blade are imposed. It is shown by Dang *et al.* [17] that the mass-averaged tangential velocity is dependent on the specific work of blades. So these choices of target design prescription allow the designer to control the blade work distribution and the overall flow field effectively. It also prevents the generation of unrealistic blades, as the designer directly controls the blade thickness.

The current viscous inverse method is applied for the inverse design of a two-dimensional blade. For two-dimensional incompressible flows the mass-averaged tangential velocity equals the mass-averaged y-directed velocity i.e.

$$\tilde{V}_{\mathrm{y}} = \frac{\int_0^s V_y \cdot V_x\,\mathrm{d}s}{\int_0^s V_x\,\mathrm{d}s} \tag{2}$$

where s denotes the blade pitch, $\tilde{V}_y$ is the mass-averaged y-directed velocity, V_x is the axial velocity, and V_y is the normal velocity. The inverse design approach computes a blade shape based

DOI: 10.1002/fld

on this target design parameter. In order to determine the required geometrical modification to accomplish the target design specification, the following steps are carried out: First, the mass-averaged tangential velocity of an initial blade is calculated using flow analysis algorithm. Then, the difference between the target and the initial mass-averaged tangential velocity is used for blade modification using blade modifying algorithm. The next step is to adapt the mesh to the modified blade. The linear tension spring analogy, which is a very fast and robust method, is applied for mesh movement during blade modification. The modified blade is then considered as an initial blade and this procedure is carried out iteratively until the differences between the target and initial mass-averaged tangential velocity are negligible. In short, the method consists of the following three steps: the viscous flow analysis, the blade modification, and the unstructured mesh movement.

2. FLOW ANALYSIS ALGORITHM

For steady incompressible viscous flow in a Cartesian coordinate system the conservation laws of mass and momentum are described by the following equations:

$$\frac{\partial}{\partial x_i}(u_i)=0 \tag{3}$$

$$\frac{\partial}{\partial x_j}\left[\rho u_i u_j-\mu\left(\frac{\partial u_i}{\partial x_j}+\frac{\partial u_j}{\partial x_i}\right)\right]=-\frac{\partial p}{\partial x_i} \tag{4}$$

where u is velocity vector, p is pressure, μ is viscosity, and ρ is density.

The primitive variables are split into their fluctuating and time-averaged components i.e.

$$u=U+u' \tag{5}$$

$$p=P+p' \tag{6}$$

where U and P are the time-averaged components and u' and p' are the fluctuating components of velocity and pressure, respectively. Substituting Equations (5) and (6) into Equations (3) and (4) and taking the time average of each equation and applying the Boussinesq hypothesis for closure of the equations yields the following equations:

$$\frac{\partial}{\partial x_i}(U_i)=0 \tag{7}$$

$$\frac{\partial}{\partial x_j}\left[\rho U_i U_j-(\mu+\mu_t)\left(\frac{\partial U_i}{\partial x_j}+\frac{\partial U_j}{\partial x_i}\right)\right]=-\frac{\partial P}{\partial x_i} \tag{8}$$

The standard k–ε model is implemented for turbulence modelling. This model is one of the most common among turbulence models that have been used in most turbomachinery CFD codes for reasons of numerical stability and also having a good compromise in terms of accuracy and robustness. In this model, μ_t is turbulent viscosity and is given by

$$\mu_t=\rho C_\mu \frac{k^2}{\varepsilon} \tag{9}$$

DOI: 10.1002/fld

An approximate transport equation for k and ε can be written in the following form:

$$\frac{\partial \rho U_i k}{\partial x_i} = \frac{\partial}{\partial x_i}\left(\frac{\mu_t}{\sigma_k}\frac{\partial k}{\partial x_i}\right) + G_k - \rho\varepsilon \tag{10}$$

$$\frac{\partial \rho U_i \varepsilon}{\partial x_i} = \frac{\partial}{\partial x_i}\left(\frac{\mu_t}{\sigma_\varepsilon}\frac{\partial \varepsilon}{\partial x_i}\right) + C_1\frac{\varepsilon}{k}G_k - C_2\rho\frac{\varepsilon^2}{k} \tag{11}$$

Here G_k represents the generation of k and is defined as

$$G_k = \mu_t\left(\frac{\partial U_i}{\partial x_j} + \frac{\partial U_j}{\partial x_i}\right)\frac{\partial U_i}{\partial x_j} \tag{12}$$

Based on experimental data from a variety of turbulent flows, Launder and Spalding [18] recommended the following values for the empirical constant that appear in Equations (10) and (11): $C_1 = 1.44$, $C_2 = 1.92$, $C_\mu = 0.09$, $\sigma_k = 1$, and $\sigma_\varepsilon = 1.3$.

The pressure correction method developed by Patankar [19] has been used to solve the incompressible Navier–Stokes equations on unstructured meshes. A cell-centred finite volume discretization of the governing equation based on the work of Mathur and Murthy [20] was developed. The second-order discretizations of the convective and diffusive terms in the governing equations are used [13]. In order to simulate turbulent flow near solid walls, the wall function approach, which is a practical and robust option for industrial flow simulations, is utilized. The implementation of wall functions is based on the method of Launder and Spalding [21]. In this approach, instead of resolving the viscous sub-layer, semi-empirical formulas called wall functions are used to bridge the viscosity-affected region between the wall and the fully turbulent region. The efficiency and accuracy of the current incompressible flow analysis algorithm have been validated for various complex geometries such as axial stator and rotor [11, 13], marine propeller [22], and turbomachinery cascades [13]. The results of the numerical calculations are in good agreement with the published data. These data are both experimental and numerical and consequently facilitated a comparison not only with the real flow patterns but also against other codes that have been developed for the solution of the Navier–Stokes equations.

3. MESH MOVEMENT ALGORITHM

Mesh movement algorithm is also an integral part of the current inverse design method. Once the blade surface is modified by inverse algorithm, the corresponding triangular mesh also needs to be changed. One approach to change the mesh for new blade is to regenerate the entire mesh from the scratch using a mesh generator code. This is of course not acceptable in terms of the required CPU time. Mesh movement is an alternative approach that is very fast and applicable in the inverse design methodology.

The mesh movement algorithm is based on the method of Batina [23], who proposed a mesh movement method based on the linear tension spring analogy. In this method, each unstructured meshes edges is modelled as springs with the stiffness inversely proportional to the length of the edges. By the displacement of the boundaries of the domain, the spring forces are calculated. Then the displacement of every interior vertex is solved iteratively until all forces are in equilibrium. A linear tension spring analogy is applied here because only the nodal displacements are important

DOI: 10.1002/fld

and not the purely elasticity variables such as local stress or strains. Also this method is a robust method with a low computational cost.

4. BLADE MODIFYING ALGORITHM BASED ON SPECIFICATION OF MASS-AVERAGED TANGENTIAL VELOCITY

The discrepancies between the specified mass-averaged tangential velocity and the actual mass-averaged tangential velocity distribution determine the geometrical blade modification. As explained in Section 3, the wall functions are used to model the flow near the solid wall region in the flow analysis algorithm. In this approach, instead of resolving the viscosity-affected inner region (viscous sub-layer and buffer layer), wall functions are used to bridge the viscosity-affected region between the wall and the fully turbulent region. So the first node near the wall is positioned outside the viscous sub-layer. Therefore, in the inverse design algorithm instead of tangential velocity along the solid walls and neglecting the boundary layer, the tangential velocity outside the viscous sub-layer is used for blade modification. The velocity at the first node near the wall, which is calculated by flow analysis code, is used in the design algorithm. In this method, it is assumed that flow does not separate. However, since a good design should not have large separation, the design method can be used for designing real turbomachinery blade.

The blade surface can be defined by the following equation:

$$\alpha^{\pm} = f \pm \frac{t_\theta}{2} \tag{13}$$

Here t_θ is the blade thickness and f is the camber line. As shown in Figure 2, all terms in Equation (13) are dependent on the x coordinate.

As an approximation the flow can be considered tangent at the edge of sub-layer of boundary layer so:

$$V^{\pm} \cdot \nabla \alpha'^{\pm} = 0 \tag{14}$$

Here $V^{\pm}$ represents the velocity on the upper and lower surface of the sub-layer of boundary layer, $\alpha'^{\pm}$ is the surface around the edge of viscous sub-layer, and $\nabla \alpha'^{\pm}$ represents the vector normal to this surface. However, the thickness of the sub-layer is usually negligible in comparison with $\alpha^{\pm}$ so:

$$\alpha'^{\pm} \approx \alpha^{\pm} \tag{15}$$

Therefore, Equation (14) yields the following equations:

$$V_x^+ \frac{\mathrm{d}\left(f + \frac{t_\theta}{2}\right)}{\mathrm{d}x} = V_y^+ \tag{16}$$

$$V_x^- \frac{\mathrm{d}\left(f - \frac{t_\theta}{2}\right)}{\mathrm{d}x} = V_y^- \tag{17}$$

DOI: 10.1002/fld

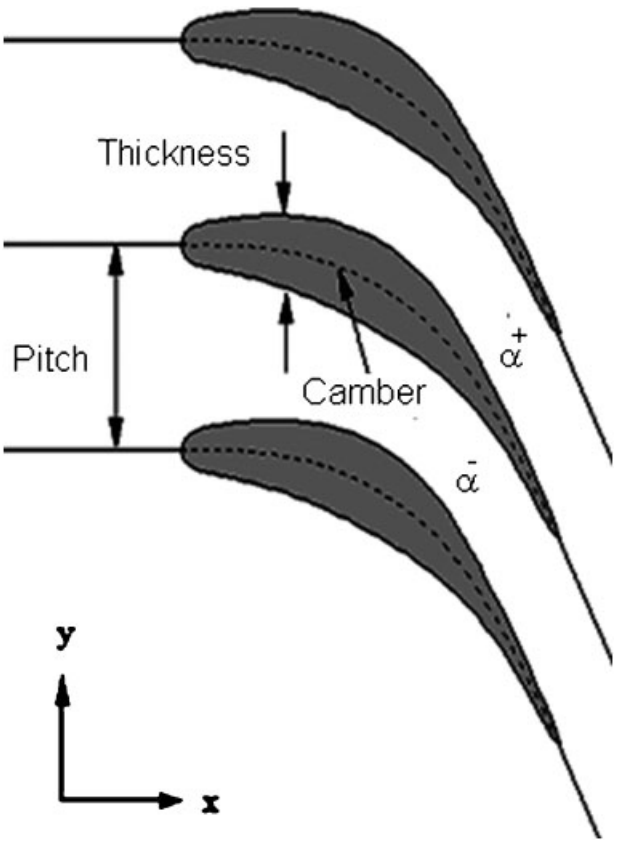

Figure 2. The two-dimensional blade cascade.

Now, applying Equations (16) and (17) to an initial camber, f^{old} , and adding Equation (16) to (17) gives

$$(V_x^{+\text{old}} + V_x^{-\text{old}})\frac{\mathrm{d}f^{\text{old}}}{\mathrm{d}x} + \frac{\mathrm{d}t_\theta}{\mathrm{d}x}\left(\frac{V_x^{+\text{old}} - V_x^{-\text{old}}}{2}\right) = V_y^{+\text{old}} + V_y^{-\text{old}} \tag{18}$$

where superscript old corresponds to the flow field computed for the blade shape obtained from the camber, f^{old}. Defining the normal and tangential blade averaged velocities (V_{ybl} and V_{xbl}) and blade difference velocity (ΔV_x) as follows:

$$V_{xbl} = \frac{(V_x^+ + V_x^-)}{2} \tag{19}$$

$$V_{ybl} = \frac{(V_y^+ + V_y^-)}{2} \tag{20}$$

$$\Delta V_x = (V_x^+ - V_x^-) \tag{21}$$

DOI: 10.1002/fld

Equation (18) can be expressed as

$$V_{xbl}^{\text{old}}\frac{\mathrm{d}(f^{\text{old}})}{\mathrm{d}x}+\frac{1}{4}\frac{\mathrm{d}t_\theta}{\mathrm{d}x}\cdot\Delta V_x^{\text{old}}=V_{ybl}^{\text{old}} \tag{22}$$

For the design problem, a correction is introduced in the right-hand-side of Equation (22) to signal a change in the blade camber. Because the objective of this method is to achieve the target mass-averaged velocity, the correction is defined as the difference between the target mass-averaged tangential velocity and the current mass-averaged tangential velocity. So, the geometrical modification is made directly proportional to the design discrepancy and a first approximate for the new camber geometry, f^{new}, following Soulis [24], will be

$$V_{xbl}^{\text{old}}\frac{\mathrm{d}(f^{\text{new}})}{\mathrm{d}x}+\frac{1}{4}\frac{\mathrm{d}t_\theta}{\mathrm{d}x}\cdot\Delta V_x^{\text{old}}=V_{ybl}^{\text{old}}+\tilde{V}_y^{*}-\tilde{V}_y^{\text{old}} \tag{23}$$

were $\tilde{V}_y^{*}$, $\tilde{V}_y^{\text{old}}$ are the target and initial mass-averaged tangential velocity, respectively. By deducting Equation (22) from Equation (23) the following equation is derived:

$$V_{xbl}^{\text{old}}\frac{\mathrm{d}(f^{\text{new}}-f^{\text{old}})}{\mathrm{d}x}=\tilde{V}_y^{*}-\tilde{V}_y^{\text{old}} \tag{24}$$

where V_{xbl} is calculated at the edge of the viscous sub-layer. All terms in Equation (24) are dependent on the x coordinate. Equation (24) is rearranged to give the camber line displacement as follows:

$$\frac{\mathrm{d}(\nabla f)}{\mathrm{d}x}=\frac{\tilde{V}_y^{*}-\tilde{V}_y^{\text{old}}}{V_{xbl}^{\text{old}}} \tag{25}$$

where

$$\nabla f=f^{\text{new}}-f^{\text{old}} \tag{26}$$

∇f is the camber line displacement after every design iteration. The derivative in Equation (25) is written in the following finite difference form:

$$\frac{\nabla f_i-\nabla f_{i-1}}{\Delta x}=\frac{\tilde{V}_y^{*}-\tilde{V}_y^{\text{old}}}{V_{xbl}^{\text{old}}} \tag{27}$$

where Δx is the horizontal distance between point (i) and point $(i-1)$ on the camber line.

To solve Equation (27), an initial condition is required. The initial condition is given by a stacking point that remains fixed throughout the iterative design procedure. Thus, for the stacking point $(i=0)$, the camber line displacement during design iterations is zero i.e.

$$\nabla f_0=0 \tag{28}$$

In the case of United Technologies Research Centre (UTRC) blade in this study, the stacking point is placed at the leading edge of the blade. Using this initial condition, the displacement at any nodes on the camber line and thus f^{new} during design iteration is calculated by Equation (27). The new blade shape is defined by adding the specified tangential thickness symmetrically to a new camber line. The design solution converges when it reaches a certain tolerance. The flowchart of the design method is shown in Figure 3.

DOI: 10.1002/fld

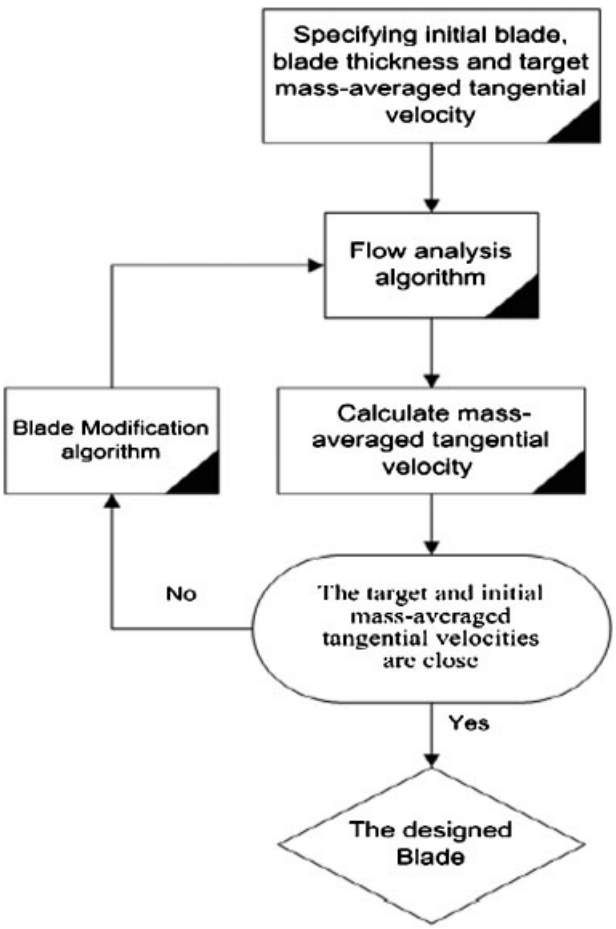

Figure 3. The flowchart of the inverse procedure.

Inverse blade design methods are now used in industry to improve the performance of a known blade or to create a new design based on earlier design which operates under the same conditions [13, 25]. Borges [16] designed a new blade using an inviscid inverse method based on the prescription of mass-averaged tangential velocity. He then constructed and investigated the performance and efficiency of the new blade. However, to assess the robustness and efficiency of inverse design methods, they can be applied to the re-design of blades for which the experimental data is available.

5. INVERSE DESIGN APPLICATION

To assess the capability and robustness of the current method and its convergence to a unique solution, it is applied to the re-design of the mid-span of a UTRC rotor blade. The data published

DOI: 10.1002/fld

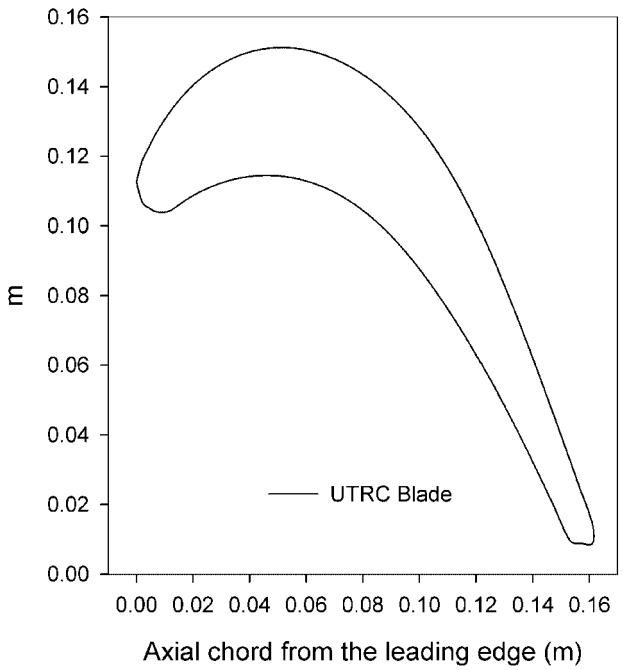

Figure 4. The blade geometry.

by [26] based on the experimental measurements of the rotor at the UTRC are used as the target design in this study. To re-design the blade, an arbitrary blade is considered as the initial blade. The UTRC blade thickness and mass-averaged tangential velocity distribution are then specified. The target is to re-design the UTRC blade using these initial and specified design parameters. The blade geometry and the computational domain are shown in Figures 4 and 5, respectively.

Figure 6 shows the triangular mesh around the initial rotor and designed blade surface. The mesh contains 13 436 triangular cells. In order to simulate the nominal operating rotational speed of the rotor, a constant tangential velocity of 29.5 m/s is specified in the flow computation. The axial flow velocity is 22.86 m/s, which is the same as the axial velocity in the experiment.

As shown in Figure 3, the discrepancies between the target and calculated mass-averaged tangential velocity determine the geometrical blade modification. Figures 7 and 8 show the geometries and mass-averaged tangential velocity of the initial, target, and redesigned blades. The results show an excellent agreement between the UTRC blade and the designed blade. The solution converges only after 65 calls to the analysis algorithm. As shown in Figure 9, the surface pressures of the designed blades and the original blade also match very closely. The blade shape converges when the maximum discrepancy between the target and calculated mass-averaged velocity reduced to 1%. The current method is more expensive in terms of the CPU cost than the method based on inviscid inverse method. Inviscid inverse design methods particularly those based on potential flow equations are very fast and may design a blade in few minutes based on the current PC performances. However, these methods are usually applied for the design of high-speed turbomachinary blades where the Reynolds numbers are very high and consequently the boundary layers are very thin. In such situations, these thin boundary layers are ignored and it is assumed that the flow

DOI: 10.1002/fld

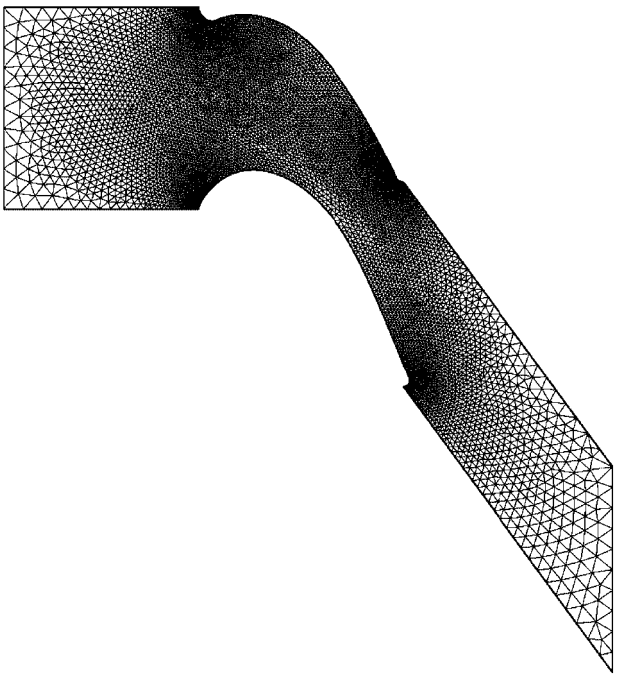

Figure 5. The mesh around the initial rotor in the complete computational domain.

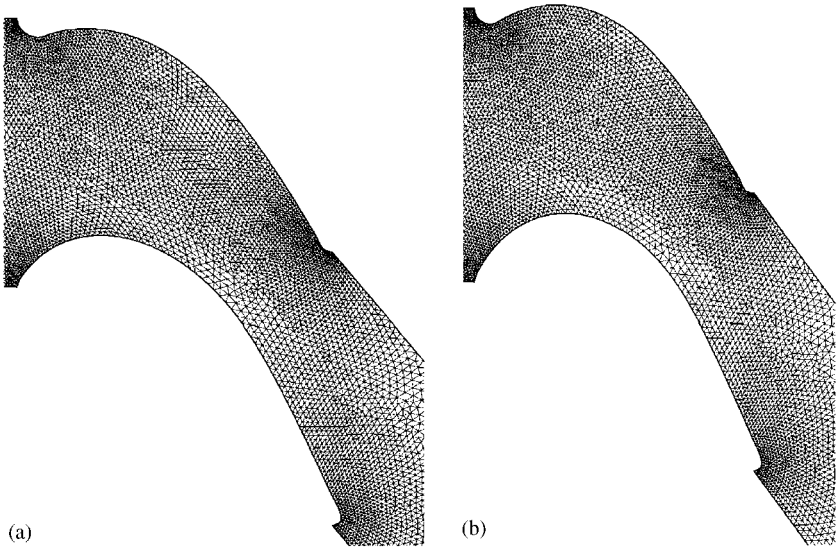

Figure 6. The close-up of mesh around (a) the initial and (b) designed blade.

DOI: 10.1002/fld

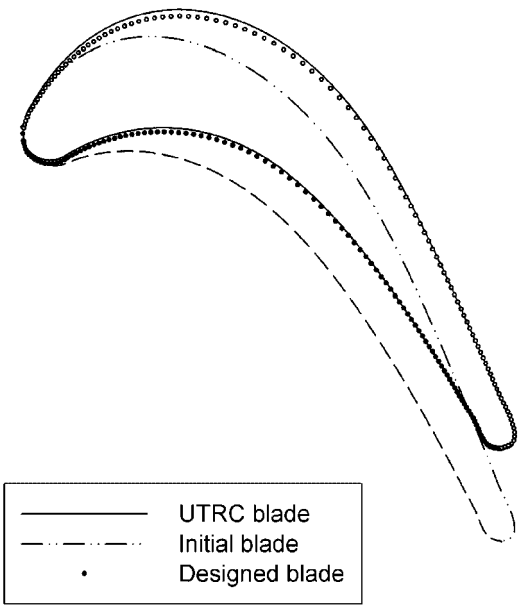

Figure 7. The initial, target, and designed blade.

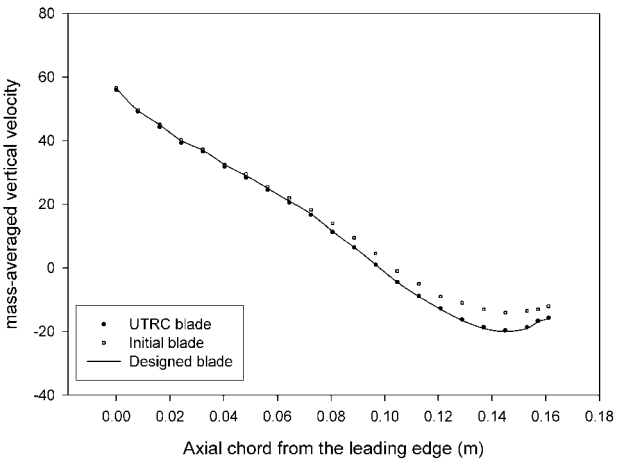

Figure 8. The initial, target, and designed mass averaged tangential velocity.

through the blades is inviscid irrotational flow. However, it is not always possible to anticipate the effects of this assumption on the performance of the turbomachinery blades. So, the flow filed through the designed blades is analysed using a flow analysis code based on the Navier–Stokes equations at the final stage of design to check the validity of this assumption and the real performance of the turbo-machinery blades. The current inverse design method is applied for redesign of a low-speed turbomachinery blade, where the viscosity and turbulence have significant effects

DOI: 10.1002/fld

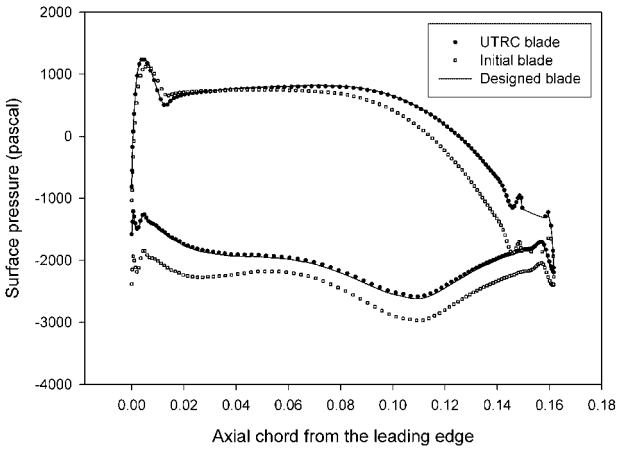

Figure 9. The surface pressure of the initial, designed, and UTRC rotor blade.

on the performance of turbomachinery. Although the method is the most expensive in terms of CPU cost among those available, no further higher-order flow analysis code is required at the final stage of the inverse design.

6. CONCLUSIONS

A novel Navier–Stokes inverse design method based on the specification of mass-averaged tangential velocity is presented. In this method, the blade shape is designed subject to a specified distribution of mass-averaged tangential velocity and the blade thickness. One of the advantages of the method is that by controlling mass-averaged tangential velocity, the specific work can be controlled as it is directly dependent on the work of a turbomachinery blade or marine propeller.

The majority of inverse design methods are based on the specification of the blade surface pressure. These methods cannot be extended to three-dimensional flows for practical applications [11]. Also in these methods defining a target pressure distribution on the blade that leads to a physically realistic blade or any blade at all cannot be guaranteed as shown by Rahmati [11]. As the present inverse design methods are based on the specification of mass-averaged tangential velocity and the blade thickness specifications it does not have the difficulties associated with design based on the specification of surface pressure.

Also one of the improvements of the present methods over previous methods is that the flow is not assumed to be inviscid. Indeed the flow field is treated as a viscous turbulent flow using a RANS model.

The capabilities of this design methodology have been verified by reproducing the mid-section of the UTRC rotor blade operating in subsonic flow region. By specifying a target mass-averaged tangential velocity with blade thickness, the final blade was successfully reproduced. The numerical results show the efficiency of the method for blade inverse design. The current study provides a strong foundation for the development of three-dimensional viscous inverse design methods and using RANS models based on unstructured meshes in design algorithms.

DOI: 10.1002/fld

REFERENCES

1. Denton JD. Calculation of three dimensional flow through any type of turbomachines. *AGARD Lecture Series*, vol. 140, NATO, Paris, 1985.
2. Jennions IK, Turner MG. Three-dimensional Navier–Stokes computations of transonic fan flow using an explicit flow solver and an implicit solver. *Journal of Turbomachinery* 1993; **15**:261–272.
3. Lakshminarayana B. *Fluid Dynamics and Heat Transfer of Turbomachinery*. Wiley: New York, 1996.
4. Obayashi S, Takanashi S. Genetic optimisation of target pressure distributions for inverse design methods. *AIAA Journal* 1996; **34**:881–886.
5. Yiu C, Zangeneh M. A 3D automatic optimization method for turbomachinery blade design. *AIAA Journal of Propulsion and Power* 2000; **16**:1174–1181.
6. Lighthill MJ. A new method of two dimensional aerodynamics design. *Aeronautical Research Council*, *London R&M*, 2112, 1945.
7. Sobieczky H, Fung NJ, Seebass AR. New method for designing shock-free transonic configuration. *AIAA Journal* 1978; **17**:722–729.
8. Zangeneh M. A compressible three-dimensional design method for radial and mixed flow turbomachinery blades. *International Journal for Numerical Methods in Fluids* 1991; **13**:599–624.
9. Demeulenaere A, Braembussche RVD. Three-dimensional inverse method for turbomachinery blading design. *Journal of Turbomachinery—Transactions of the ASME* 1998; **120**:247–255.
10. Dang T, Jiang J. Design method for turbomachine blades with finite thickness by the circulation method. *Journal of Turbomachinery* 1997; **119**:539–543.
11. Rahmati MT. Incompressible Navier–Stokes inverse design method based on unstructured meshes. *Ph.D. Thesis*, University College London, London, 2006.
12. Takanashi S. Iterative three-dimensional transonic wing design using integral equations. *Journal of Aircraft* 1985; **22**:655–660.
13. Rahmati MT, Charlesworth D, Zangeneh M. Incompressible Navier–Stokes inverse design method based on adaptive unstructured mesh. *The 13th Annual Conference on Computational Fluid Dynamics*, St. John's, Canada, 2005.
14. Dang T. A fully three-dimensional inverse method for turbomachinery blading in transonic flows design. *ASME Journal of Turbomachinery* 1993; **115**:354–361.
15. Hawthrone WR, Wang C, Tan CS, McCune JE. Theory of blade design for large deflections, Part I: two dimensional cascade. *Journal of Engineering for Gas Turbines and Power—Transactions of the ASME* 1984; **106**:346–353.
16. Borges JE. A three-dimensional inverse method for turbomachinery, Part I. *Journal of Turbomachinery—Transactions of the ASME* 1990; **112**:346–354.
17. Dang T, Damle S, Qiu X. Euler-based inverse method for turbo-machine blade, Part 2: three-dimensional flows. *AIAA Journal* 2000; **38**(11):207–213.
18. Launder BE, Spalding DB. *Lectures in Mathematical Models of Turbulence*. Academic Press: London, 1972.
19. Patankar SV. *Numerical Heat Transfer and Fluid Flow*. Taylor & Francis: U.S.A., 1980.
20. Mathur SR, Murthy YT. A pressure-based method for unstructured meshes. *Numerical Heat Transfer*, *Part B* 1997; **31**:195–215.
21. Launder BE, Spalding DB. The numerical computation of turbulent flows. *Computer Methods in Applied Mechanics and Engineering* 1974; **3**:269–289.
22. Rahmati MT. A RANS code for flow simulation of marine propellers. *The International Conference on Computer Applications in Shipbuilding*, Portsmouth, U.K., September 2007.
23. Batina JT. Unsteady Euler airfoil solutions using unstructured dynamic meshes. *AIAA Journal* 1990; **28**(8): 1381–1388.
24. Soulis JV. Thin turbomachinery blade design using a finite volume method. *International Journal for Numerical Methods in Engineering* 1985; **21**:19–36.
25. Hu P, Choo B, Zangeneh M, Rahmati M. On design of transonic fan rotors by 3D inverse design method. *ASME Paper GT2006-91173*, 2006.
26. Dring RP, Joslyn HD, Hardin LW, Wagner JH. Turbine rotor–stator interaction. *ASME* 82-GT-3, 1982.

DOI: 10.1002/fld